

para-carbon atoms and attached methyl groups listed in Table I are very close to those of diamagnetic metalloporphyrins.<sup>20</sup> The signal at 166.8 ppm is that of a proton-bearing carbon atom, and the signal is split (167.3 and 163.1 ppm) for the *m*-tolyl analogue, thus indicating the ortho-carbon assignment. A non-proton-bearing carbon signal at 127.7 ppm is assigned to the remaining quaternary phenyl carbon atom. Although porphyrin carbon-13 signals follow general Curie-law behavior, poor solubility of the five-coordinate complexes at low temperature precluded a complete temperature dependence study.

Spectra for (OEP)Fe and (ETIO)Fe complexes were recorded in both CH<sub>2</sub>Cl<sub>2</sub> and C<sub>6</sub>H<sub>6</sub> solvents at temperatures from 16 to 55 °C. (Slow oxidation of the iron(II) species was noted for the chlorinated solvent.) Spectral assignments are listed in Table I. Pyrrole carbon assignments are based on the ordering observed for the (TPP)Fe species. Further analogy to the (TPP)Fe complexes suggested that the meso-carbon signal of (OEP)Fe(1,2-MeIm) and (ETIO)Fe(1,2-MeIm) would be near the diamagnetic value (~97 ppm). This is indeed the case, as the 94.2-ppm signal for the (OEP)Fe complex was resolved as a doublet in the proton-coupled spectrum. Proton coupling patterns for the 100.3- and 44.8-ppm signals also permitted respective assignments to the CH<sub>2</sub> and CH<sub>3</sub> groups.

Although the solutions prepared for carbon-13 spectral studies contained excess 1,2-dimethylimidazole, no resonances corresponding to free ligand positions were noted. Small, sharp signals such as the one at -3.4 ppm in Figure 1a were detected, however. The positions of these signals were strongly dependent on the relative amounts of free and coordinated ligand. Thus, rapid ligand exchange on the carbon-13 NMR time scale was suggested, much as was previously discerned for proton NMR measurements.<sup>6,7</sup> Poor solubility precluded "freezing out" ligand exchange at low temperatures. Accordingly, the coordinated ligand chemical shift values were estimated from experiments where 1,2-dimethylimidazole was added in excess, and it was assumed that the observed ligand chemical shifts were mole fraction weighted with respect to concentrations of free and coordinated ligand. Solutions were examined that contained 0.01 M ((*m*-CH<sub>3</sub>)TPP)Fe and either 0.10 or 0.25 M 1,2-dimethylimidazole. Reasonable agreement between calculated values for these two solutions supports the assumption of dynamics at the near-fast-exchange limit. Estimated chemical shift values for coordinated 1,2-dimethylimidazole are listed in Table I.

Large downfield pyrrole carbon shifts are expected for the high-spin d<sup>6</sup> configuration as a consequence of strong interaction between the  $\sigma$ -type d<sub>x<sup>2</sup>-y<sup>2</sup> unpaired spin and pyrrole nitrogen atoms. Likewise, large downfield shifts for imidazole 2- and 4-carbon atoms are likely due to unpaired spin in the d<sub>z<sup>2</sup></sub> orbital. Effects of  $\pi$ -type spin delocalization from unpaired spin in the d<sub>xz</sub>, d<sub>yz</sub> set are less evident for the high-spin iron(II) porphyrins than for corresponding five-coordinate high-spin iron(III) complexes. Thus, the iron(III) derivatives exhibit pyrrole carbon signals in the 1200-1300-ppm region.<sup>16-19</sup> The pyrrole  $\beta$ -carbon signal is broader than the pyrrole  $\alpha$ -carbon signal of high-spin iron(III) porphyrins. This is likely a consequence of large  $\pi$  unpaired spin density delocalized through the 3e( $\pi$ ) molecular orbital<sup>17</sup> (which has larger amplitude at the pyrrole  $\beta$ -carbon atom<sup>21</sup>). Reversal of pyrrole carbon line widths and smaller isotropic shift values for high-spin iron(II) complexes are indicative of smaller  $\pi$  spin density contributions. The pyrrole ethyl carbon atoms of (OEP)Fe species also reflect the degree of  $\pi$  spin delocalization, which should give the CH<sub>2</sub> resonance an upfield bias and</sub>

the CH<sub>3</sub> resonance a downfield shift. This effect is apparent in CH<sub>2</sub> and CH<sub>3</sub> signals of 100.3 and 44.8 ppm for (OEP)-Fe(1,2-MeIm) vs. respective values of 75.0 and 149.0 ppm for (OEP)FeCl.<sup>14</sup>

The meso-carbon signal of ((*p*-CH<sub>3</sub>)TPP)Fe(1,2-MeIm) exhibits a downfield shift (isotropic shift) of only 5.7 ppm when compared with that for a diamagnetic cobalt(III) analogue.<sup>20</sup> In terms of the spin delocalization pattern, this small meso-carbon shift is deceptive. Thus, isotropic shifts for the attached phenyl carbon, the ortho carbon, and the meso proton (of the (OEP)Fe complex) are -9.6, +33, and -9 ppm, respectively. The pattern of alternating shift direction is reminiscent of that for five-coordinate high-spin iron(III) complexes,<sup>16-19</sup> although shifts are approximately an order of magnitude greater for the higher oxidation state species. This shift pattern may be described by a polarization mechanism in which positive  $\pi$  spin density at the meso-carbon atom induces  $\sigma$ -type spin density in attached phenyl groups. The relatively small  $\pi$  spin density at the meso-carbon atom reasonably reflects a minor contribution of spin delocalization through the 4e( $\pi^*$ ) MO (which exhibits large amplitude at the meso-carbon position<sup>21</sup>). Controversy over interpretation of previous proton NMR results has centered on the degree of  $\pi$  spin delocalization in high-spin iron(II) porphyrins.<sup>6,7</sup> Carbon-13 spectroscopy provides a better view of the entire macrocycle, and it may safely be stated that  $\pi$  spin density in high-spin iron(II) porphyrins is a fraction of that in iron(III) analogues. Attenuation of pyrrole carbon shifts also implies diminished  $\sigma$  spin delocalization in iron(II) vs. iron(III) porphyrins. The apparent importance of electrostatic interactions will be investigated by carbon-13 methods for other metalloporphyrin species.

In more empirical terms, the model study presented here provides a basis for carbon-13 NMR examination of deoxy-hemoproteins and also strategy for carbon-13 label incorporation into the macromolecules. Porphyrin ring methyl and methylene as well as meso-carbon and imidazole 5-carbon signals should be found in the 90-100-ppm region, reasonably isolated from the bulk of protein signals. Unfortunately, the potential overlap of these several paramagnetic signals will complicate assignments. Signals far downfield of the diamagnetic region are expected for pyrrole carbon atoms and for the imidazole 2-carbon and 4-carbon signals. Severe line broadening will likely preclude observation of these resonances in the absence of label incorporation.

**Acknowledgment.** Support from NIH Grant GM28831-02 is gratefully acknowledged.

**Registry No.** ((*p*-CH<sub>3</sub>)TPP)Fe(1,2-MeIm), 83547-71-1; ((*m*-CH<sub>3</sub>)TPP)Fe(1,2-MeIm), 83547-72-2; (OEP)Fe(1,2-MeIm), 75811-16-4; (ETIO)Fe(1,2-MeIm), 83547-73-3.

Contribution from the Département de Recherches Physiques (LA 71), Université Pierre et Marie Curie, 75230 Paris Cedex 05, France, Laboratoire de Chimie (LA 32), Ecole Normale Supérieure, 75231 Paris Cedex 05, France, and Institut de Chimie (LA 31), Université Louis Pasteur, 67008 Strasbourg, France

### Resonance Raman Spectra of Metalloporphyrins with a Ligand Inserted between the Metal and a Pyrrole Nitrogen

G. Chottard,\*<sup>1a</sup> D. Mansuy,<sup>1b</sup> and H. J. Callot<sup>1c</sup>

Received May 18, 1982

Resonance Raman (RR) spectroscopy has been successfully used in recent years to gain insight into the structure of he-

(20) Goff, H. M. *J. Am. Chem. Soc.* **1981**, *103*, 3714.

(21) LaMar, G. N.; Walker, F. A. In "The Porphyrins"; Dolphin, D., Ed.; Academic Press: New York, 1979; Vol. IV, pp 61-157.

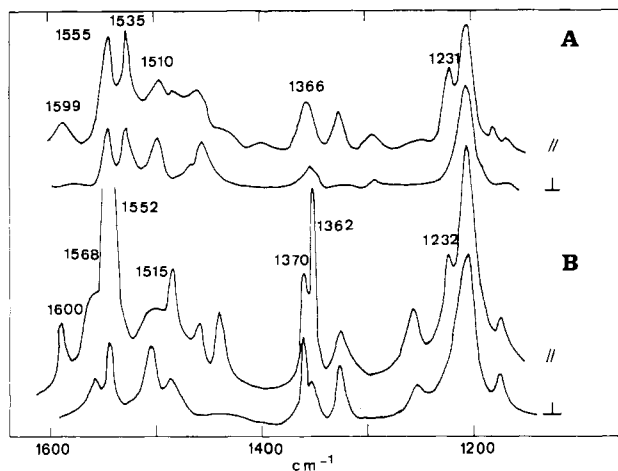
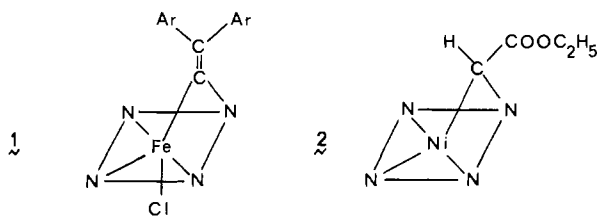


**Figure 1.** RR spectra of (A) complex **1** and, (B) Fe(TPP)Cl in CHCl<sub>3</sub>, with complex concentration 10<sup>-3</sup> M and λ<sub>0</sub> = 514.5 nm (60 mW). Polarization of the scattered light is either parallel (//) or perpendicular (⊥) to the polarization of the incident light.

moproteins. Structural implications of the frequencies of the prominent Raman bands have been well established,<sup>2,3</sup> and a growing number of iron-axial ligand vibrations have been observed.<sup>4</sup> Hemoprotein (Hp) derivatives and their model compounds have in common an iron-porphyrin chromophore (Fe-P), which is usually considered as belonging to the D<sub>4h</sub> or C<sub>4v</sub> point groups, and so far RR spectra have been only described for Hp or Fe-P complexes displaying these types of symmetry. However, more asymmetric structures of the active site of Hp have been proposed for intermediate states in enzymatic cycles. For example, an Fe<sup>III</sup>-P complex, with a carbenic ligand inserted into one of the Fe-N bonds, has been proposed recently as a carbon analogue of compound **1** of catalase.<sup>5,6</sup> This complex exhibits a highly distorted porphyrin ring and an unusual pure intermediate spin state of the iron ( $S = 3/2$ ).<sup>7</sup>

We report here the RR spectrum of this compound, Fe(TPP)[C=C(p-Cl-HC<sub>6</sub>H<sub>4</sub>)<sub>2</sub>](Cl) (**1**), together with that of Ni(TPP)(CHCOOC<sub>2</sub>H<sub>5</sub>) (**2**), another metalloporphyrin with a carbenic ligand inserted into a Ni-N bond,<sup>9</sup> and discuss their characteristic features by comparison with metalloporphyrins of fourfold symmetry.



### Experimental Section

Compounds **1** and **2** were prepared according to already described procedures.<sup>9,10</sup>

- (1) (a) Université Pierre et Marie Curie. (b) Ecole Normale Supérieure. (c) Université Louis Pasteur.
- (2) Spiro, T. G.; Burke, J. M. *J. Am. Chem. Soc.* **1976**, *98*, 5482.
- (3) Chottard, G.; Battioni, P. Battioni, J. P.; Lange, M.; Mansuy, D. *Inorg. Chem.* **1981**, *20*, 1718.
- (4) Carey, P. R.; Salares, V. R. *Adv. Infrared Raman Spectrosc.* **1980**, *7*, 1.
- (5) Chevrier, B.; Weiss, R.; Lange, M.; Chottard, J. C.; Mansuy, D. *J. Am. Chem. Soc.* **1981**, *103*, 2899.
- (6) Latos, Grazynski, L.; Cheng, R. J.; La Mar, G. N.; Balch, A. L. *J. Am. Chem. Soc.* **1981**, *103*, 4270.
- (7) Mansuy, D.; Morgenstern-Badarau, I.; Lange, M.; Gans, P. *Inorg. Chem.* **1982**, *21*, 1427.
- (8) TPP = dianion of tetraphenylporphyrin.
- (9) Callot, H. J.; Tschamber, T.; Chevrier, B.; Weiss, R. *Angew. Chem., Int. Ed. Engl.* **1975**, *14*, 567.

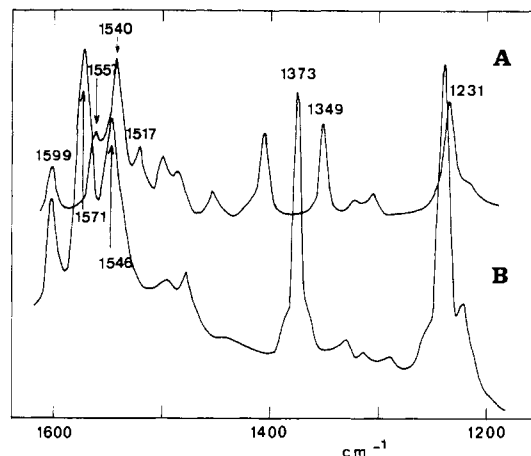


**Figure 2.** RR spectra of (A) complex **2** and (B) Ni(TPP) in CHCl<sub>3</sub>, with complex concentration 10<sup>-3</sup> M and λ<sub>0</sub> = 457.9 nm (20 mW).

**Table I.** RR Frequencies (1600-1200 cm<sup>-1</sup>) of Inserted-Ligand Metalloporphyrins **1** and **2** vs. Those of Regular Fourfold Symmetry Metalloporphyrins

marker band	Fe <sup>III</sup> . (TPP)(Cl)	complex 1	Ni(TPP)	complex 2
C <sub>6</sub> H <sub>5</sub> p	1600	1599	1601	1599
E dp	1568	1555	1580	1557
D p	1552	1535	1571	1540
C ap	1515	1510	1546	1517
p	1495	1492	1494	1495
p	1471	1470	1477	1484
p	1453			1446
p				1404
B dp	1370			
A p	1362	1366	1373	1349
			1364	
ap	1335	1336	1330	1319
		1307		1303
dp	1268	1270		
C <sub>6</sub> H <sub>5</sub> p	1232	1231	1236	1231

Raman spectra were measured in C<sub>6</sub>H<sub>6</sub> and CHCl<sub>3</sub> solutions at 10<sup>-3</sup> M concentration, with use of a rotating cell. A Coderg double monochromator was used, with Ar<sup>+</sup> and Kr<sup>+</sup> laser excitation. The slit width is 5 cm<sup>-1</sup>, and the frequencies are accurate within ±1.5 cm<sup>-1</sup>.

### Results

The RR spectra of compounds **1** and **2** are shown respectively in Figures 1 and 2, together with those of typical fourfold symmetry porphyrins: complex **1** is compared to Fe(TPP)Cl, another Fe<sup>III</sup> porphyrin with the same coordination number, though a different spin, and complex **2** is compared to Ni(TPP), another four-coordinated Ni porphyrin. The main Raman frequencies of these compounds are listed in Table I. These data show a significant lowering of the two highest Raman frequencies of the porphyrin ring (labeled D and E) in the case of the insertion compounds: the 1568- and 1552-cm<sup>-1</sup> bands of Fe(TPP)Cl are shifted to 1555 and 1535 cm<sup>-1</sup> for complex **1** and the 1580- and 1571-cm<sup>-1</sup> bands of Ni(TPP) are shifted to 1561 and 1544 cm<sup>-1</sup> for complex **2**.

This trend is followed by other Raman modes of the porphyrin, namely, the 1520-cm<sup>-1</sup> anomalously polarized vibration, and the 380-cm<sup>-1</sup> polarized mode. The vibrations of the meso phenyl groups are not affected (see, for example, the 1600- and 1230-cm<sup>-1</sup> modes).

Other features associated with the Raman spectra of ligand-inserted porphyrins **1** and **2** are as follows: (i) appearance of new but weak vibrational modes below 1000 cm<sup>-1</sup>; (ii)

- (10) Mansuy, D.; Lange, M.; Chottard, J. C. *J. Am. Chem. Soc.* **1979**, *101*, 6437.

smooth repartition of the intensity among the various vibrational modes, with visible as well as Soret excitation; (iii) dispersion of the depolarization ratios. For example, the depolarization ratio of the 1535-cm<sup>-1</sup> mode of complex **1** varies from 0.4 at 454.5 nm to 0.6 at 514.5 nm and 0.75 at 530.8 nm whereas the depolarization ratio of the 1552-cm<sup>-1</sup> mode of Fe(TPP)Cl is 0.12 at 454.5 and 514.5 nm, in agreement with the expected value of 0.125 for a polarized mode in *D*<sub>4h</sub> symmetry. The comparison is not so striking in the case of complex **2**, as there is already some dispersion for the vibrations of Ni(TPP) itself, this molecule having the *S*<sub>4</sub> symmetry.<sup>11</sup>

### Discussion

Complex **1** possesses only one plane of symmetry, thus belonging to the *C*<sub>s</sub> point group, and complex **2** has no element of symmetry. This drastic departure from fourfold symmetry does not show up on the absorption spectra: no splitting of the  $\alpha\beta$  bands is observed in the Ni series (**2**,  $\lambda_{\max}(\alpha\beta)$  615 (sh) and 548 nm, in *C*<sub>6</sub>H<sub>6</sub>; NiTPP,  $\lambda_{\max}$  525 nm), while the hyper character of the spectra of the Fe<sup>III</sup> complexes already precludes such an observation. The symmetry lowering is expected to alter the Raman spectra in the following ways: the number of vibrational modes should increase, as the out-of-plane modes of *E*<sub>g</sub> symmetry become RR active, and the depolarization ratios should become dependent on the excitation frequencies, as the symmetric and antisymmetric invariants are mixed in low-symmetry groups. Actually these features are observed in the spectra of complexes **1** and **2** and thus are a mere consequence of the lowering of symmetry.

Dispersion of the depolarization ratios renders more difficult the assignment of the spectrum of the Fe insertion complex in terms of marker bands, A, B, C, and D.<sup>3</sup> Let us recall that the occurrence of B (dp) and the frequency of band D (p) are dependent on the presence of a pentacoordinated species<sup>3</sup> whereas the frequencies of band A (p) and C (ap) are sensitive to both the spin and oxidation states of the iron according to ref 12 or mostly to the spin according to ref 3. Bands A and C may still be clearly identified with use of the following criteria: intensity enhancement with blue excitation for band A and depolarization ratio higher than 0.75 for band C.

Linear relationships have been proposed linking band C frequency to the core radius of metalloporphyrins.<sup>3,13</sup> They cannot be used for such distorted structures as the ones considered here. A more complete equation has been derived in which  $\nu_c$  frequency is linked to both the core radius and the tilt of the pyrroles.<sup>14</sup> It does not seem relevant here, inasmuch as each pyrrole unit is tilted differently over the mean 4 N plane.<sup>5,9</sup> From a qualitative point of view one may notice that the  $\nu_c$  frequency of complex **1** is among the lowest measured for this band. In agreement with this finding, though a core radius cannot be strictly defined, a rather large mean value of 2.10 Å is obtained from the C<sub>i</sub>...N<sub>1</sub>(N<sub>2</sub>, N<sub>3</sub>) and C<sub>i</sub>...N<sub>4</sub> distances, calculated by triangulation from the X-ray data.<sup>5</sup> For complex **2** a higher value is measured for  $\nu_c$  and a lower "core radius" (2.07 Å) is calculated from X-ray data.<sup>15</sup>

Previous RR studies of Fe(TPP) derivatives<sup>3,12</sup> have emphasized the role of spin in the determination of the Raman frequencies, so that one may question our choice of Fe(TPP)(Cl) as a reference compound. The RR data available for intermediate-spin derivatives<sup>16-18</sup> show that they are closer

to those of low-spin than those of high-spin complexes. Accordingly the choice as a reference of a low-spin hexacoordinated Fe<sup>III</sup> complex such as Fe(TPP)(Im)<sub>2</sub>Cl or of a low-spin pentacoordinated Fe<sup>II</sup> complex such as Fe(TPP)(CS) would have been relevant too. With use of RR data of these reference compounds<sup>3,12</sup> the lowering of the high-frequency doublet would be even more important.

The C<sub>β</sub>-C<sub>β</sub> and C<sub>α</sub>-C<sub>m</sub> stretches are predominant in the high-frequency modes.<sup>19</sup> Though the C<sub>β</sub>-C<sub>β</sub> and C<sub>α</sub>-C<sub>m</sub> bond lengths of complexes **1** and **2** are not different from those of regular *D*<sub>4h</sub> metalloporphyrins, the tilt of one pyrrole unit (N<sub>4</sub>) brings the corresponding C<sub>β</sub>-C<sub>β</sub> bond out of the mean 4 N plane (for example, in complex **2**, dihedral angles between the 4 N plane and pyrroles N<sub>1</sub>-N<sub>4</sub> are respectively 13.3, 5.9, 3.6, and 46.4°).<sup>15</sup> Thus, the  $\pi$  conjugation within the macrocycle is decreased; as a consequence, the corresponding vibrational frequencies are decreased.

In summation, occurrence of new vibrational modes below 1000 cm<sup>-1</sup>, dispersion of the depolarization ratios, and frequency lowering of the two highest porphyrinic vibrational modes are characteristic features of the RR spectra of ligand-inserted metalloporphyrins. Studies are under way to show that those features are to be expected whenever one of the pyrroles is severely tilted.

Registry No. **1**, 79311-02-7; **2**, 55822-49-6.

- (17) Kitagawa, T.; Osaki, Y.; Kyogoku, Y.; Horio, T. *Biochim. Biophys. Acta* **1977**, *495*, 1.  
 (18) Ogoshi, H.; Sugimoto, H.; Yoshida, Z. *Biochim. Biophys. Acta* **1980**, *621*, 19.  
 (19) Abe, M.; Kitagawa, T.; Kyogoku, Y. *J. Chem. Phys.* **1978**, *69*, 4526.

Contribution from the Department of Chemistry, Texas A&M University, College Station, Texas 77843

### Oxidation of 2,6-Di-*tert*-butylphenol by Molecular Oxygen. Catalysis by Tetrakis(bipyridyl)( $\mu$ -peroxo)( $\mu$ -hydroxo)dicobalt(III)

Stephen A. Bedell<sup>1</sup> and Arthur E. Martell\*

Received April 27, 1982

The active sites in metalloenzymes contain coordinated metal ions in a molecular environment that is favorable for the formation of dioxygen complexes that may be involved as intermediates in biological oxidations.<sup>2</sup> For example, cytochrome P-450 enzymes contain iron porphyrin complexes similar to those functioning as oxygen carriers in the transport and storage proteins hemoglobin and myoglobin.<sup>3</sup> Recent studies of the active sites of tyrosinase, responsible for the hydroxylation of tyrosine, suggest an active center able to bind dioxygen to copper in a binuclear fashion.<sup>4</sup> A binuclear copper(I) model has also been suggested as the active site of the arthropod oxygen-transport protein hemocyanin.<sup>5</sup>

Models for such oxidation catalysts generally involve the "end-on",  $\sigma$ -type complexes, because of their similarity to dioxygen-binding complexes in biological systems. The cobalt-Schiff's base-dioxygen complex systems have been the

- (11) Hoard, J. L. In "Porphyrins and Metalloporphyrins"; Smith, K. M., Ed.; Elsevier: Amsterdam, 1975.  
 (12) Burke, J. M.; Kincaid, J. R.; Peters, S.; Gagne, R. R.; Collman, J. P.; Spiro, T. G. *J. Am. Chem. Soc.* **1978**, *100*, 6083.  
 (13) Huong, P. V.; Pommier, J. C. *C.R. Hebd. Seances Acad. Sci., Ser. C* **1977**, *285*, 519.  
 (14) Spiro, T. G.; Stong, J. D.; Stein, P. *J. Am. Chem. Soc.* **1979**, *101*, 2648.  
 (15) Chevrier, B.; Weiss, R. *J. Am. Chem. Soc.* **1976**, *98*, 2985.  
 (16) Streckas, T. C.; Spiro, T. G. *Biochem. Biophys. Acta* **1974**, *351*, 237.

- (1) Abstracted in part from a dissertation to be submitted by Stephen A. Bedell to the Faculty of Texas A&M University in partial fulfillment of the requirements for the degree of Doctor of Philosophy.  
 (2) Hamilton, G. A. "Molecular Mechanisms of O<sub>2</sub> Activation"; Hayaishi, O., Ed.; Academic Press: New York, 1974; p 405.  
 (3) Ullrich, V. *Top. Curr. Chem.* **1979**, *83*, 67.  
 (4) Winkler, M. E.; Lerch, K.; Solomon, E. K. *J. Am. Chem. Soc.* **1981**, *103*, 7001.  
 (5) Freedman, T. B.; Loehr, J. S.; Loehr, T. M. *J. Am. Chem. Soc.* **1976**, *98*, 2809.